



Contents lists available at ScienceDirect

Saudi Journal of Biological Sciences

journal homepage: [www.sciencedirect.com](http://www.sciencedirect.com)

Original article

# High-throughput screening to identify potential inhibitors of the Z $\alpha$ domain of the adenosine deaminase 1 (ADAR1)

Hani Choudhry\*

Department of Biochemistry, Faculty of Science, Cancer and Mutagenesis Unit, King Fahd Medical Research Center, King Abdulaziz University, Jeddah, Saudi Arabia



## ARTICLE INFO

### Article history:

Received 11 January 2021

Revised 26 June 2021

Accepted 27 June 2021

Available online 1 July 2021

### Keywords:

High-throughput screening

ADAR1

Epi

Molecular dynamics

Molecular simulations

ADAR inhibitors, cancer

## ABSTRACT

Adenosine deaminases acting on RNA 1 (ADAR1) are enzymes involved in editing adenosine to inosine in the dsRNAs of cells associated with cancer development. The p150 isoform of ADAR1 is the only isoform containing the Z $\alpha$  domain that binds to both Z-DNA and Z-RNA. The Z $\alpha$  domain is suggested to modulate the immune response and could be a suitable target for antiviral treatment and cancer immunotherapy. In this study, we aimed to identify potential inhibitors for ADAR1 protein that bind the Z $\alpha$  domain using molecular docking and simulation tools. Virtual docking and molecular dynamics simulation approaches were used to screen the potential activity of 2115 FDA-approved compounds on the Z $\alpha$  domain of ADAR1 and filtered for to obtain the top-scoring hits. The top three compounds with the best XP Gscore—namely alendronate (−7.045), etidronate (−6.923), and zoledronate (−6.77)—were subjected to 50 ns simulations to characterize complex stability and identify the fundamental interactions that contribute to inhibition of the ADAR1 Z $\alpha$  domain. The three compounds were shown to interact with Lys169, Lys170, Asn173, and Tyr177 of the Z $\alpha$  domain-like helical backbone of Z-RNA. The study provides a comprehensive and novel insights of repurposes drugs for the inhibition of ADAR1 function.

© 2021 The Author(s). Published by Elsevier B.V. on behalf of King Saud University. This is an open access article under the CC BY-NC-ND license (<http://creativecommons.org/licenses/by-nc-nd/4.0/>).

## 1. Introduction

RNA editing involving the conversion of adenosine to inosine (A-to-I editing) is considered the most predominant epigenetic modification in eukaryotes (Fritzell, et al. 2018; Peng, et al. 2018; Wulff & Nishikura, 2010). To date, millions of editing sites have been detected in humans using inosine chemical erasing sequencing (ICE-seq) (Suzuki, Ueda, Okada, & Sakurai, 2015). A-to-I editing RNA modifications are frequently found in Alu double-stranded RNAs (Alu dsRNAs) located in introns and untranslated regions (UTRs) (Nishikura, 2010). A-to-I editing is catalyzed by adenosine deaminase acting on RNA (ADAR) enzymes; these enzymes usually catalyze dsRNAs of 20 bp in length (Ishizuka, et al. 2019). When adenosine is converted to inosine in the mRNA's coding region, this

could change the amino acid sequence of the coded protein in what is called a re-coding editing event. A-to-I editing could also either create or eliminate splice sites on pre-mRNA transcripts, potentially affecting mRNA posttranscriptional maturation and processing (Fritzell, et al. 2018).

The three major ADARs studied in eukaryotes are ADAR1, ADAR2, and ADAR3; of these, ADAR1 is the most prevalent and is ubiquitously expressed (Nishikura, 2016). The function of ADAR1 involves the editing of adenosine to inosine in the RNA of cells associated with the immune response and nervous impulses. ADAR1 is involved in the regulation of innate immune response by editing specific sites for the easy interpretation and recognition of host (or self) and non-self RNAs; i.e., ADAR1 is reported to inhibit the replication of hepatitis C and human immunodeficiency virus (HIV) by editing their RNA (Clerzius, et al. 2013; Doria, et al. 2009; Hartwig, et al. 2006). In addition, ADAR1 controls the function of neurotransmitters in the nervous system by editing the coding sites of the receptor proteins that interact with neurotransmitters (Behm & Öhman, 2016).

The mutation or altered expression of ADAR1 is associated with human diseases such as infantile encephalopathy Aicardi–Goutières syndrome (AGS) and cancer. Several studies have identified the aberrant expression of ADAR1 in several cancers including breast cancer, chronic myeloid leukemia (CML), lung cancer, liver

\* Corresponding author at: Biochemistry Department, Cancer and Mutagenesis Unit, Faculty of Sciences, King Abdulaziz University, P.O. Box.80203, Jeddah 21589, Saudi Arabia.

E-mail address: [hchoudhry@kau.edu.sa](mailto:hchoudhry@kau.edu.sa)

Peer review under responsibility of King Saud University.



cancer, and melanoma. The overexpression of ADAR1 in several cancers is correlated with tumorigenesis and cancer progression (Amin, et al. 2017; Chen, et al. 2013; Chen, et al. 2017; Kung, et al. 2020; Zipeto, et al. 2016).

Recently, ADAR1 was reported to be overexpressed in breast cancer. Breast cancer cell survival depends on the p150 isoform of ADAR1. The knockdown of ADAR1 weakens cell proliferation and tumorigenesis through activation of the interferon (IFN) signaling pathway and apoptosis, as reported in triple-negative breast cancer (TNBC) (Kung, et al. 2020). Similarly, ADAR1 expression in breast cancer was shown to positively regulate dihydrofolate reductase (DHFR) activity through editing of miR-125a-3p and miR-25-3p binding sites that interact with the 3' UTR of DHFR, thereby enhancing cell proliferation and increasing methotrexate resistance (Kung, et al. 2020; Nakano, et al. 2017). Consistent with this study, CML, liver cancer, lung cancer, and bladder cancer were shown to exhibit increased levels of ADAR1 (Nakano, et al. 2017).

In liver cancer, ADAR1 edits the mRNA transcripts of antizyme inhibitor 1 (AZIN1), leading to changes in amino acid from serine (Ser) to glycine (Gly) which, in turn, increases the binding ability of AZIN1 to antizymes, thereby preventing the antizyme-mediated degradation of cyclin D1 and ornithine decarboxylase. Increased levels of cyclin D1 and ornithine decarboxylase promote cell proliferation and tumor progression (Chen, et al. 2013).

There are two isoforms of ADAR1, called p150 and p110. Both p150 and p110 have the deaminase (catalytic) domain, three-stranded RNA binding domain, and Z $\beta$  domain. Only p150 has the Z $\alpha$  domain (Athanasiadis, 2012; Placido, et al. 2007). The p150 isoform is predominantly found in the cytoplasm and is induced by interferon, whereas p110 is located in the nucleus and is constitutively produced. In p150, the Z $\alpha$  domain binds to both Z-RNA and Z-DNA, confirming that both RNA and DNA are similarly suited as ligands of Z $\alpha$ . Evidence has pointed toward the regulatory role of the Z $\alpha$  domain of ADAR1 in immune response through the double stranded RNA sensing via MDA5/MAVS/IRF3/IFN axis (Herbert, 2019; Koeris, et al. 2005). This mechanism has recently been exploited in targeting viral infection and for cancer immunotherapy purposes. In this study, we aimed to identify potential inhibitors for ADAR1 protein using molecular docking and simulation tools.

## 2. Materials and methods

### 2.1. Preparation of molecules

A total of 2115 approved compounds were obtained from the ZINC database, and the molecules were downloaded in mol2 format and then uploaded to Maestro software -Schrödinger Release 2020. The LigPrep -Released 2017 and EpiK interfaces of the Maestro suite were used for molecule preparation; using the OPLS3e force field (Roos, et al. 2019), 2627 conformations were generated.

### 2.2. Preparation of ADAR1 Z $\alpha$ domain

The crystal structure of the Z-alpha (Z $\alpha$ ) domain of the RNA-editing enzyme ADAR1 bound by the left-handed RNA double helix (PDB ID:2GX8) was obtained from RCSB Protein Data Bank (PDB), and hydrogen atoms were added, zero bond orders to metal were created and other hetero atoms were deleted. Ionization states were generated at a pH of 7.0  $\pm$  2.0 using EpiK in Maestro (Roos, et al. 2019). Eventually, water molecules were removed, and protein energy was minimized using the OPLS3e force field (Roos, et al. 2019).

### 2.3. Binding site prediction

The SiteMap interface of Maestro was used for binding site prediction; the selection of the active site was based on the site's exhibited interaction with the RNA double helix, as shown in the obtained crystal structure (PDB ID:2GX8)

### 2.4. Virtual screening and docking protocols

The high-throughput virtual screening (HTVS) docking of Maestro was used to screen the FDA-approved compounds for possible inhibitors of the Z $\alpha$  domain of ADAR1. The top 200 hits were further docked using standard precision (SP) and extra precision (XP) docking protocols to determine the molecules' final poses with better docking energy and their types of interactions. The protein was set as rigid, and the ligand was flexible. The scaling factor and partial charge cutoff of the van der Waals radii of ligand atoms were specified to be 0.80 and 0.15, respectively. Final scoring of the energy-minimized poses was carried out and displayed as a Glide score and XP docking score. Finally, the 20 best docked poses with extra precision docking and with the lowest Glide score values were recorded. The docking complexes were viewed and analyzed using the Protein-Ligand Interaction Profiler (PLIP) web server.

### 2.5. Molecular dynamics (MD) simulation for ADAR1

MD simulation was performed to determine the strength of protein-ligand interaction, as previously described (Rehman, et al. 2019). Three ligand-protein complexes with the lowest XP docking energy and greatest number of bonds were selected for 50 ns MD simulation using DESMOND (Desmond, Schrödinger, LLC, New York, NY, USA). An orthorhombic simulation box with a boundary of 10 Å was used with the TIP3P water model; six Cl atoms were added to neutralize the system. After minimization, the system was submitted to a 50 ns MD simulation that used 300 K and a 101,325 bar NPT (normal pressure and temperature) ensemble and 100 ps relaxation. The trajectories were recorded in 50 ps intervals. After job completion, the root mean square deviation (RMSD) and root mean square fluctuation (RMSF) were used to examine complex stability.

## 3. Results

### 3.1. Analysis of Z $\alpha$ /Z-RNA complex

The retrieved 3D structure of the Z $\alpha$  domain of the p150 isoform was bound by the left-handed RNA double helix (Z-RNA). The complex exhibited pi-pi stacking bonding with Tyr177 and three salt bridges with Lys: two with Lys169 and one with Lys170 (Fig. 1).

### 3.2. Z $\alpha$ domain binding site prediction

The SiteMap interface predicted the active site of the Z $\alpha$  domain in Maestro, which identified Thr157, Ala158, His159, Lys169, Asn173, Pro192, Pro193, and Trp195 as residues representing the active site; the same residues are associated with the interaction of the RNA double helix (Fig. 1). The druggability (Dscore) of the catalytic pocket of the protein was 0.38, and the site score was 0.6. Usually, sites with Dscore  $\geq$  1.0 are classified as very druggable, a Dscore of 0.8–1.0 classified as druggable, Dscore of 0.7–0.8 indicating intermediate druggability, and Dscore  $\leq$  0.7 indicating limited druggability (Ghantas, et al. 2016). Even though the Z $\alpha$  domain is classified as having poor druggability, the subsequent steps of docking and molecular dynamic simulation showed the possibility of preventing Z $\alpha$ /Z-RNA bonds. Molecular docking and

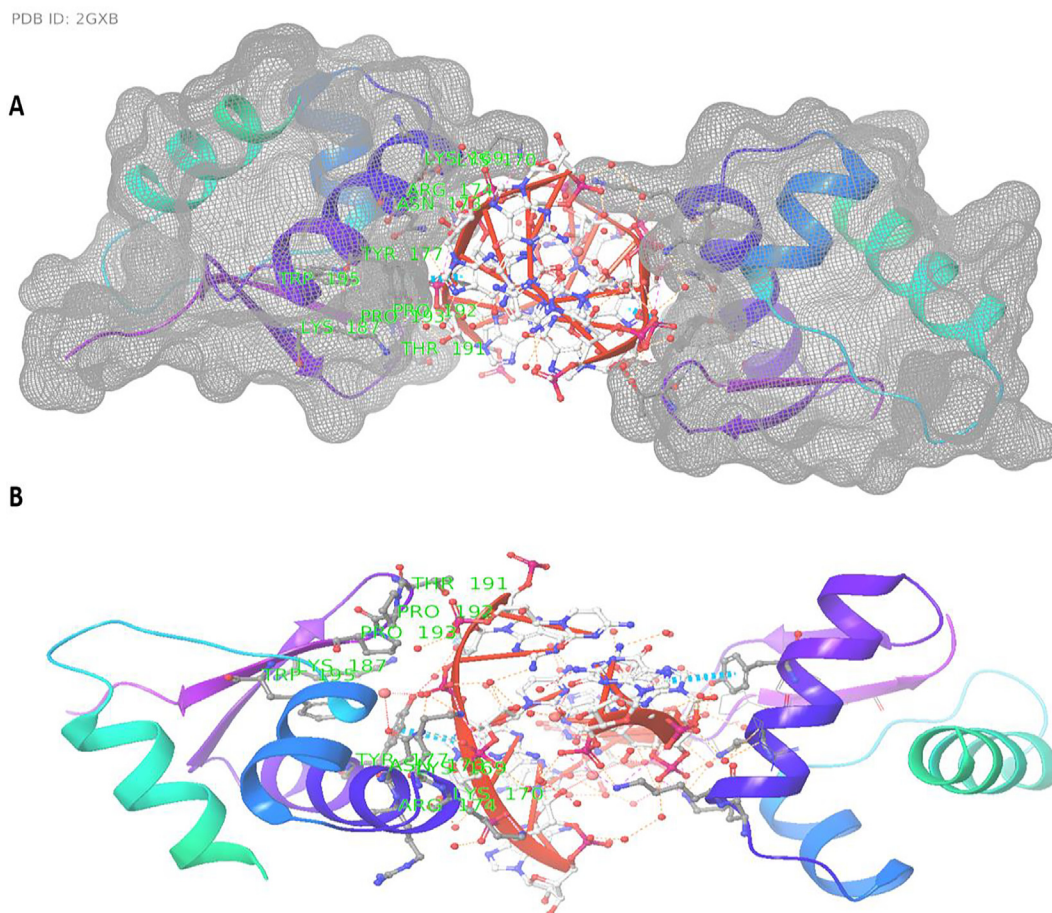


**Fig. 1.** A and B show the 3D structures of the Z $\alpha$  domain of the RNA-editing enzyme adenosine deaminases acting on RNA 1 (ADAR1) bound by the left-handed RNA double helix in the center (PDB: 2GXB).

MD simulation are methods widely used for detecting protein inhibitors (Rehman, et al. 2019).

### 3.3. Virtual screening and molecular docking of the top-three potential ADAR1 inhibitors based on the Z $\alpha$ /Z-RNA complex

Virtual screening was performed on 2627 compounds, and the best 200 compounds binding to the Z $\alpha$  domain with the highest glide score were chosen for SP and XP docking. The top 50 compounds with the highest XP Gscore due to the interaction of Z $\alpha$  are shown in Table 1, and the structure of these compounds is illustrated in Fig. 2. The best three compounds with the highest scores were further analyzed. Alendronate (ZINC00003801919), a drug used to prevent bone loss, had the best XP Gscore of  $-7.045$  and had the best stable interaction during docking

and simulation. The stability was maintained through four hydrogen bonds with residues Lys169, Asn173, Tyr177, and Gly190 (Table 2) (Figs. 3 and 4A) and one hydrophobic interaction with Pro193 was also observed. The compound showed a strong H-bond with a small distance ( $1.65 \text{ \AA}$ ). This interaction could interfere with the formation of the pi-pi stacking bond which occurs between Tyr177 and double-stranded RNA. Alendronate is used to prevent and treat certain types of bone loss, and its anticancer activity on various types of cancer has been reported in previous studies (Ilyas, et al. 2019).

The docking study revealed potent activity of etidronate (ZINC00003830813) on the Z $\alpha$  domain of ADAR1, showing a low XP Gscore ( $-6.9$ ). Etidronate is a class of drugs used in the treatment of osteoporosis (Ioachimescu and Licata, 2007). Four hydrogen bonds were formed due to the interaction of etidronate and

**Table 1**  
Top 10 FDA approved compounds with docking energy and docking scores that target ADAR1.

ZINC ID	Name	XP GScore	Docking Score	Energy (kcal/mol)
ZINC00003801919	Alendronate	$-7.045$	$-6.846$	15.277156
ZINC00003830813	Etidronate	$-6.923$	$-6.677$	27.482013
ZINC00003803652	Zoledronate	$-6.77$	$-6.263$	14.44624
ZINC00000001554	Acne	$-6.327$	$-6.327$	19.397025
ZINC000085537017	Cangrelor	$-6.269$	$-6.255$	45.568277
ZINC00003812862	Pamidronate	$-6.254$	$-6.144$	12.508963
ZINC00003830813	Etidronate	$-6.381$	$-6.135$	26.317013
ZINC000001531009	Risedronate	$-6.322$	$-6.134$	35.741586
ZINC00000895081	Citrate	$-6.129$	$-6.129$	28.385779
ZINC00000000922	Pas	$-6.063$	$-6.062$	14.90494

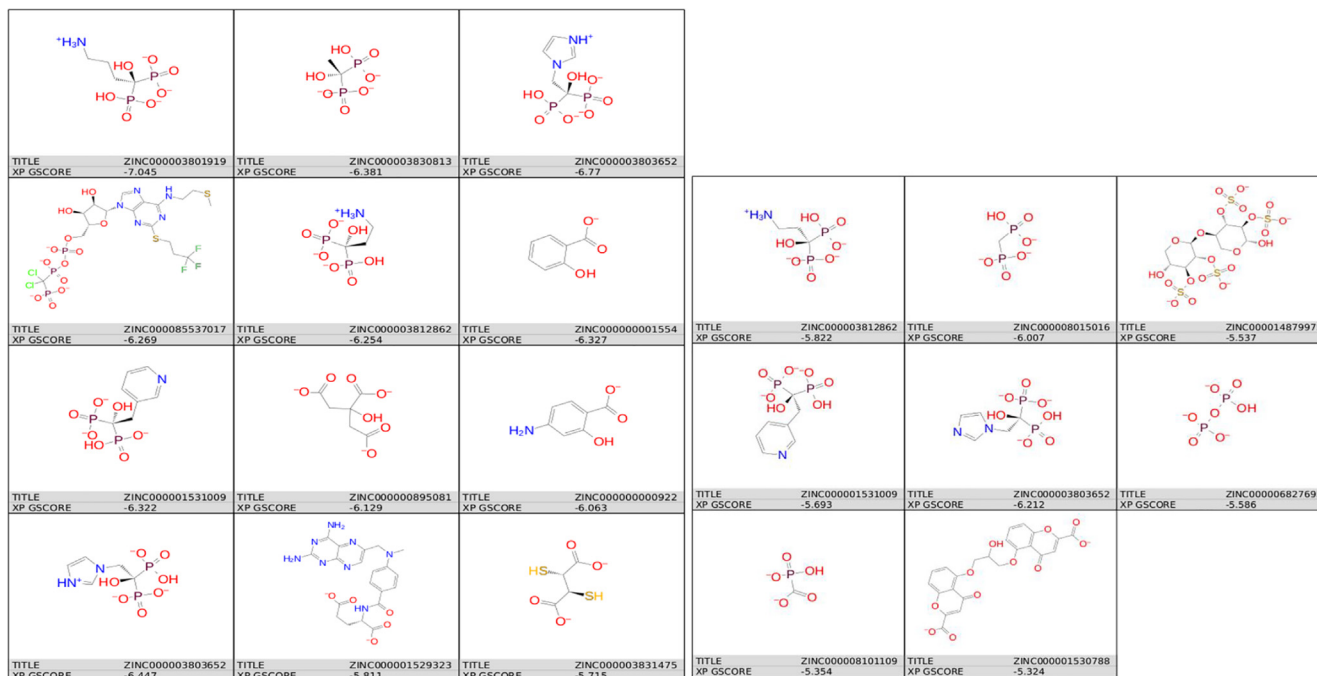


Fig. 2. Two-dimensional structures of the top 20 compounds showing an interaction with the Z $\alpha$  domain.

Table 2

Hydrogen bond interactions of amino acid residues with different ligands.

	Index	Residue	AA	Distance H–A	Donor Atom	Acceptor Atom
Alendronate	1	169A	Lys	1.82	501 [N $_3^+$ ]	1017 [O $_2$ ]
	2	173A	Asn	1.63	578 [Nam]	1018 [O $^-$ ]
	3	177A	Tyr	1.65	655 [O $_3$ ]	1013 [O $_2$ ]
	4	190A	Gly	2.79	1006 [N $_3^+$ ]	864 [O $_2$ ]
Etidronate	1	169A	Lys	1.79	501 [N $_3^+$ ]	1010 [O $_2$ ]
	2	173A	Asn	1.56	578 [Nam]	1011 [O $^-$ ]
	3	177A	Tyr	1.75	655 [O $_3$ ]	1014 [O $_2$ ]
Zoledronate	1	169A	Lys	1.94	501 [N $_3^+$ ]	1009 [O $^-$ ]
	2	173A	Asn	1.89	578 [Nam]	1021 [O $_3$ ]
	3	173A	Asn	2.23	1021 [O $_3$ ]	577 [O $_2$ ]
	4	177A	Tyr	1.77	655 [O $_3$ ]	1020 [O $^-$ ]

the Z $\alpha$  domain, with Lys169, Asn173 (two), and Tyr177 involved in this interaction (Table 2) (Figs. 3 and 4B).

Zoledronate (ZINC000003803652) forms five stable hydrogen bonds with Z $\alpha$  domain backbone residues Lys169 (two), Asn173 (two), and Tyr177. Zoledronate was able to block the essential residues (Lys169 and Tyr177) associated with RNA binding by stable hydrogen bonds, and these bonds were stabilized by its small distances (1.94 and 1.77 Å, respectively). The blocking of these two essential residues might prevent the attachment of the Z $\alpha$  domain to Z-RNA (Table 2) (Figs. 3 and 4C). These interactions were in line with the study of the Z $\alpha$ /Z-RNA complex, which showed that the Lys169, Lys170, Asn173, and Tyr177 residues of the Z $\alpha$  binding pocket interact with the RNA helical backbone, suggesting that Z-RNA could not bind to the Z $\alpha$  binding pocket when occupied by either of the top three screened compounds alendronate, etidronate, or zoledronate.

### 3.4. Molecular dynamic simulation of Alendronate, etidronate and zoledronate

MD simulation was used to analyze the conformational change of each protein and a chosen hit. The Z $\alpha$ /alendronate complex was subjected to molecular dynamics simulation for 50 ns, as shown in

Fig. 4A1. The RMSD of C-alpha was used to measure the deviation of the protein backbone during the simulation. The ligand aligned with the protein backbone until 15 ns, but after this time, the ligand separated from the protein and fluctuated in the range of 5–20 Å; then, for a short period (35–45 ns) the ligand aligned again, and in the later part of the simulation, a greater fluctuation of 12 Å was observed in the range of 6–18 ns (Fig. 4A). The large fluctuation of the ligand was attributed to the presence of seven rotatable bonds in the ligand (Fig. 5A), as the presence of a greater number of rotatable bonds will generate a greater number of fluctuations (Musyoka, et al. 2016). Several hydrogen bonds and their occupancies during the molecular dynamic simulations were determined, as shown in Fig. 4B. A similar trend of unstable interaction was observed in zoledronate, with the ligand divergent from the protein backbone during most of the simulation time (Fig. 4C). For etidronate compound, the RMSD of the protein backbone as well as the ligand during the second half of the simulation showed excellent stability; the ligand aligned with the protein, and ligand fluctuation was lower compared to alendronate. This could be due to the lower number of rotatable bonds in etidronate (Fig. 4A and 5B). Two hydrogen bonds formed between the essential residues (Lys169 and Lys170) associated with double-stranded RNA interaction, and they were stable for the whole of the simulation time. The

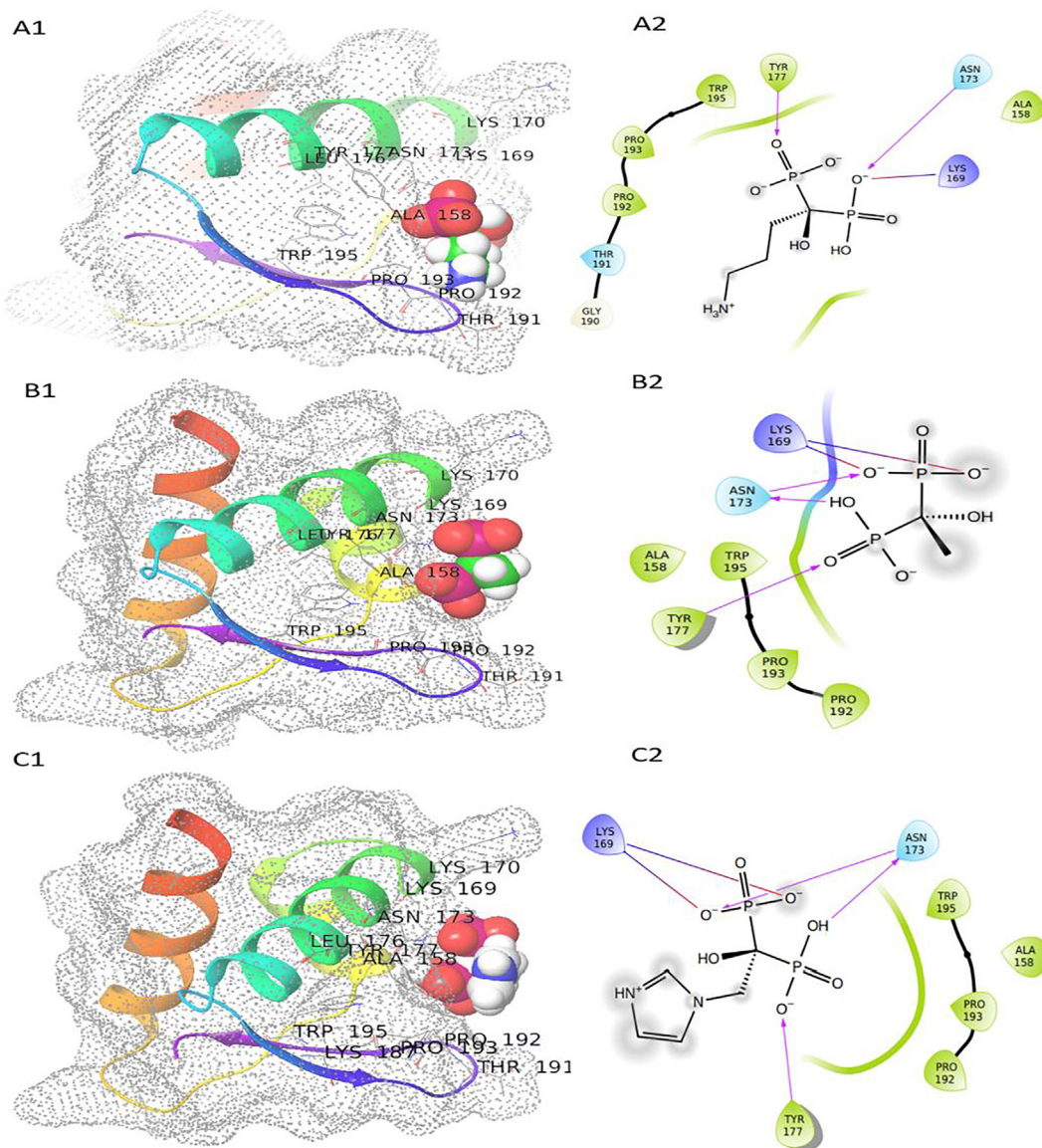


**Fig. 3.** Three and two-dimensional structures of the interaction of ligands and ADAR1 Z $\alpha$  domain. A. Interaction of the Z $\alpha$ /alendronate (ZINC000003801919) complex. B. Interaction of the Z $\alpha$ /etidronate (ZINC000003830813) complex. C. Interaction of the Z $\alpha$ /zoledronate (ZINC000003803652) complex.

stable interaction of etidronate with the Z $\alpha$  domain of ADAR1 indicates its valuable use in blocking the active site of the protein.

#### 4. Discussion

ADAR1 is an important A-to-I editing enzyme that has been determined to play a vital role in the immune response, viral infection, and cancer. The p150 isoform of ADAR1 is associated with the MDA5/MAVS/IRF3/IFN axis implicated in the immune response (Herbert, 2019). Although numerous studies have identified ADAR1 as a potential therapeutic target for viral and cancer treatment (Amin, et al. 2017; Chen, et al. 2013; Chen et al. 2017; Kung, et al. 2020; Zipeto, et al. 2016), there are currently no anti-ADAR1 drugs approved by the FDA. In the current study, we screened 2627 compounds for possible inhibitors of ADAR1 using the Z $\alpha$ /Z-RNA complex.

The Z $\alpha$  domain is a key to increase site-selectivity of the ADAR1 (p150) editing enzyme. Both Z-DNA and Z-RNA were reported to be substrates of the conserved Z $\alpha$  domain (Athanasiadis, 2012). Stud-

ies have shown that the catalytic activity of ADAR1 (p150) is altered in the presence of Z-forming substrate; this also creates changes in editing patterns, resulting in enhancement of the catalytic activity of A-to-Z-conversion in dsRNA, while ADAR1 (p150) is bound to the substrate. Therefore, the A-to-Z conformational switch at the Z $\alpha$  domain is essential for stimulating adenosine deaminase activity (Koeris, et al. 2005; Placido, et al. 2007). Based on the function of Z $\alpha$  as a modulator site of ADAR1 catalytic activity, we screened FDA-approved drugs for possible repurposing in inhibition of the Z $\alpha$  domain. Three drugs—alendronate, etidronate, and zoledronate—were selected based on their XP Gscore. Molecular interactions shown that all three drugs interact with Lys169, Lys170, Asn173, and Tyr177 of ADAR1-like Z-RNA and Z-DNA, as illustrated using X-ray crystallography (Placido et al., 2007). The molecular interactions of Z $\alpha$ /Z-RNA and Z $\alpha$ /Z-DNA complexes are identical except at position 174, containing arginine (Arg174), which is specifically found in the Z $\alpha$ /Z-RNA complex (Placido, et al. 2007). Interestingly, zoledronate showed strong hydrogen bonding and hydrophobic interactions at Arg174 (Fig. 4C), suggesting that it could be a potent inhibitor of Z $\alpha$  and

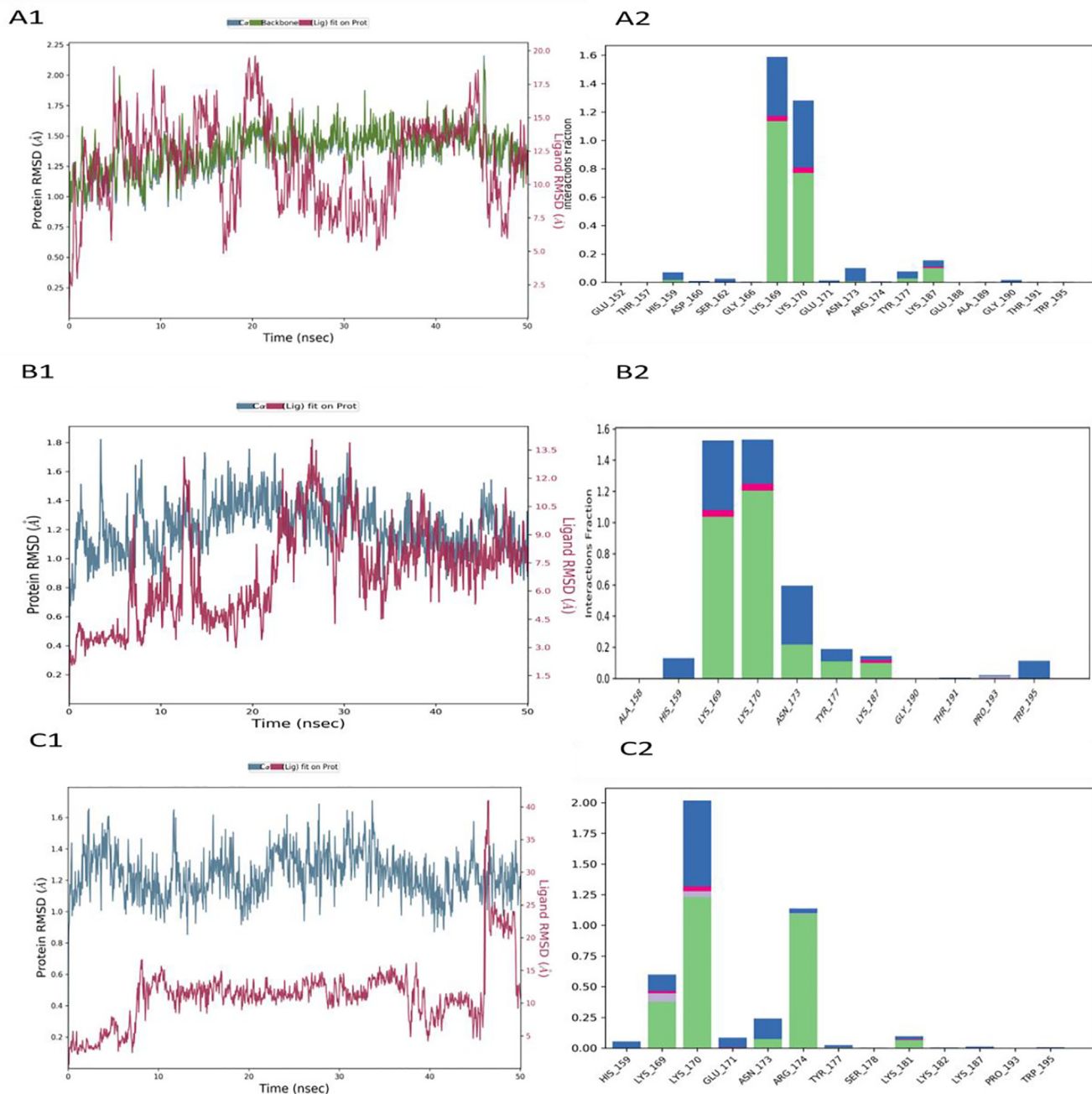


**Fig. 4.** Root mean square deviation (RMSD) and histogram (green color for hydrogen bonds, blue for water bridges) of the interaction of ligands and ADAR1  $Z\alpha$  domain during a 50 ns simulation. A. Interaction of alendronate (ZINC000003801919) and  $Z\alpha$ . B. Interaction of etidronate (ZINC000003830813) and the  $Z\alpha$  domain. C. Interaction of zoledronate (ZINC000003803652) and the  $Z\alpha$  domain.

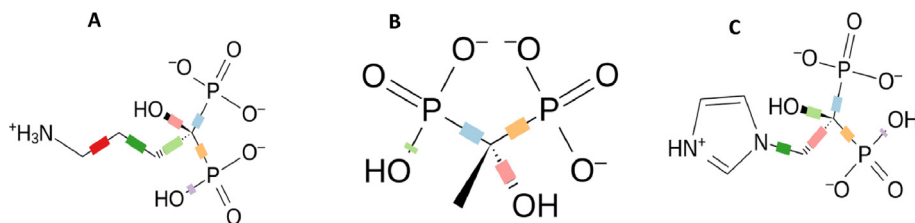


**Fig. 5.** Ligand torsions during simulation with rotatable bonds shown in different colors A. alendronate (ZINC000003801919); B. etidronate (ZINC000003830813); C. zoledronate (ZINC000003803652).

Z-RNA binding and could prevent the catalytic activity of ADAR1 in the A-to-I editing of RNA transcripts. Overall, the results demonstrate the significant stability of alendronate, etidronate, and zoledronate in the  $Z\alpha$  domain binding pocket and their dynamic stability during molecular dynamic simulation, suggesting that they could be repurposed as inhibitors of ADAR1 in the treatment of diseases associated with the overexpression of ADAR1 and A-to-I RNA editing, such as viral infection and cancer. One of the lingering problems in oncology is the ability of cancer cells to escape immunosurveillance, enabling them to go undetected at the early stage of infection (Huntington, et al. 2020). Severe cancer types with poor prognosis and a high mortality rate—i.e., breast cancer, lung cancer, CML, and liver cancer—exhibit highly overexpressed ADAR1 (Amin, et al. 2017; Chen, et al. 2013; Sagredo, et al. 2018; Yang, et al. 2017). The overall function of ADAR1 in these cancer types is to promote cancer cell proliferation, progression, and migration by evading the immune system (Ishizuka, et al. 2019). Therefore, targeting ADAR1 is important for cancer immunotherapy (Bhate, et al. 2019).

In conclusion, alendronate, etidronate, and zoledronate could be potential candidate drugs for use in a combination regimen with other anticancer drugs toward the more effective treatment of diseases characterized by overexpression or alteration of ADAR1.

## 5. Conclusion

This research provides novel insights into the inhibition of one of the key RNA-editing enzymes, ADAR1, which has a significant impact on the progression of many diseases including various cancers and immunological and viral disorders. This study performed comprehensive high-throughput *in silico* screening to identify potential inhibitors of ADAR1 and characterized their molecular interactions. The findings of this study can promote epitranscriptome drug discovery based on the molecular structure of RNA-editing enzymes.

## Funding

The author extends his appreciation to the Deputyship for Research and Innovation at the Ministry of Education in Saudi Arabia for funding this research work through the project number (871).

## Declaration of Competing Interest

The authors declare that they have no known competing financial interests or personal relationships that could have appeared to influence the work reported in this paper.

## Acknowledgment

The author acknowledges the support from the Deputyship for Research & Innovation at the Ministry of Education and the King Abdulaziz University, Jeddah, Saudi Arabia.

## References

Amin, E.M., Liu, Y., Deng, S., Tan, K.S., Chudgar, N., Mayo, M.W., Jones, D.R., 2017. The RNA-editing enzyme ADAR promotes lung adenocarcinoma migration and invasion by stabilizing FAK. *Sci. Signaling* 10 (497). <https://doi.org/10.1126/scisignal.aah3941>.

Athanasiadis, A., 2012. Zalpha-domains: At the intersection between RNA editing and innate immunity. In: *Seminars in Cell and Developmental Biology*. Elsevier Ltd. <https://doi.org/10.1016/j.semcdb.2011.11.001>.

Behm, M., and Öhman, M., 2016. RNA Editing: A Contributor to Neuronal Dynamics in the Mammalian Brain. *Trends in Genetics*. Elsevier Ltd. <https://doi.org/10.1016/j.tig.2015.12.005>

Bhate, A., Sun, T., Li, J.B., 2019. ADAR1: A New Target for Immuno-oncology Therapy. *Mol. Cell*. Cell Press. <https://doi.org/10.1016/j.molcel.2019.02.021>.

Chen, L., Li, Y., Lin, C.H., Chan, T.H.M., Chow, R.K.K., Song, Y., Guan, X.Y., 2013. Recoding RNA editing of AZIN1 predisposes to hepatocellular carcinoma. *Nat. Med.* 19 (2), 209–216. <https://doi.org/10.1038/nm.3043>.

Chen, W., He, W., Cai, H., Hu, B., Zheng, C., Ke, X., Wang, H., 2017. A-to-I RNA editing of BLCAP lost the inhibition to STAT3 activation in cervical cancer. *Oncotarget* 8 (24), 39417–39429. <https://doi.org/10.18632/oncotarget.17034>.

Clerzius, G., Shaw, E., Daher, A., Burugu, S., Gélinas, J.F., Ear, T., Gatignol, A., 2013. The PKR activator, PACT, becomes a PKR inhibitor during HIV-1 replication. *Retrovirology*. <https://doi.org/10.1186/1742-4690-10-96>.

Doria, M., Neri, F., Gallo, A., Farace, M.G., Michienzi, A., 2009. Editing of HIV-1 RNA by the double-stranded RNA deaminase ADAR1 stimulates viral infection. *Nucleic Acids Res.* <https://doi.org/10.1093/nar/gkp604>.

Fritzell, K., Xu, L. Di, Lagergren, J., & Öhman, M., 2018. ADARs and Editing: The role of A-to-I RNA modification in cancer progression. *Seminars in Cell Developmental Biology*. Elsevier Ltd. <https://doi.org/10.1016/j.semcdb.2017.11.018>

Ghattas, M., Raslan, N., Sadeq, A., Al Sorkhy, M., Atatreh, N., 2016. Druggability analysis and classification of protein tyrosine phosphatase active sites. *Drug Des. Develop. Therapy* 10, 3197–3209. <https://doi.org/10.2147/DDDT.S111443>.

Hartwig, D., Schütte, C., Warnecke, J., Dorn, I., Hennig, H., Kirchner, H., Schlenke, P., 2006. The large form of ADAR 1 is responsible for enhanced hepatitis delta virus RNA editing in interferon- $\alpha$ -stimulated host cells. *J. Viral Hepatitis*. <https://doi.org/10.1111/j.1365-2893.2005.00663.x>.

Herbert, A., 2019. ADAR and immune silencing in cancer. *Trends in Cancer*. Cell Press. <https://doi.org/10.1016/j.trecan.2019.03.004>.

Huntington, N.D., Cursons, J., Rautela, J., 2020. The cancer-natural killer cell immunity cycle. *Nat. Rev. Cancer* 1–18. <https://doi.org/10.1038/s41568-020-0272-z>.

Ilyas, N.S.A., Zarina, S., Hashim, Z., 2019. Assessment of anticancer effect of alendronate in breast cancer: an *in vitro* study. *J. Biotechnol. Biomed. Sci.* 2 (2), 1–7. <https://doi.org/10.14302/jissn.2576-6694.jbbs-19-2953>.

Ioachimescu, A., Licata, A., 2007. Etidronate: What is its place in treatment of primary osteoporosis and other demineralizing diseases today? *Current Osteoporosis Reports*. Current Med. Group LLC 1. <https://doi.org/10.1007/s11914-007-0012-2>.

Ishizuka, J.J., Manguso, R.T., Cheruiyot, C.K., Bi, K., Panda, A., Iracheta-Vellve, A., Haining, W.N., 2019. Loss of ADAR1 in tumours overcomes resistance to immune checkpoint blockade. *Nature* 565 (7737), 43–48. <https://doi.org/10.1038/s41586-018-0768-9>.

Koeris, M., Funke, L., Shrestha, J., Rich, A., Maas, S., 2005. Modulation of ADAR1 editing activity by Z-RNA *in vitro*. *Nucleic Acids Res.* 33 (16), 5362–5370. <https://doi.org/10.1093/nar/gki849>.

Kung, C.P., Cottrell, K.A., Ryu, S., Bramel, E.R., Kladney, R.D., Bao, E.A., Weber, J.D., 2020. Evaluating the therapeutic potential of ADAR1 inhibition for triple-negative breast cancer. *Oncogene*. <https://doi.org/10.1038/s41388-020-01515-5>.

Musuyoka, T.M., Kanzi, A.M., Lobb, K.A., Tasthan Bishop, Ö., 2016. Structure Based Docking and Molecular Dynamic Studies of Plasmodial Cysteine Proteases against a South African Natural Compound and its Analogs. *Sci. Rep.* 6 (1), 1–12. <https://doi.org/10.1038/srep23690>.

Nakano, M., Fukami, T., Gotoh, S., Nakajima, M., 2017. A-to-I RNA editing up-regulates human dihydrofolate reductase in breast cancer. *J. Biol. Chem.* 292 (12), 4873–4884. <https://doi.org/10.1074/jbc.M117.775684>.

Nishikura, K., 2010. Functions and Regulation of RNA Editing by ADAR Deaminases. <https://doi.org/10.1146/annurev-biochem-060208-105251>

Nishikura, K., 2016. A-to-I editing of coding and non-coding RNAs by ADARs. *Nature Reviews Molecular Cell Biology*. Nature Publishing Group. <https://doi.org/10.1038/nrm.2015.4>

Peng, X., Xu, X., Wang, Y., Hawke, D.H., Yu, S., Han, L., Mills, G.B., 2018. A-to-I RNA Editing Contributes to Proteomic Diversity in Cancer. *Cancer Cell* 33 (5), 817–828.e7. <https://doi.org/10.1016/j.ccell.2018.03.026>.

Placido, D., Brown, B.A., Lowenhaupt, K., Rich, A., Athanasiadis, A., 2007. A Left-Handed RNA Double Helix Bound by the  $Z\alpha$  Domain of the RNA-Editing Enzyme ADAR1. *Structure* 15 (4), 395–404. <https://doi.org/10.1016/j.str.2007.03.001>.

Rehman, M.T., Alajmi, M.F., Hussain, A., Rather, G.M., Khan, M.A., 2019. High-throughput virtual screening, molecular dynamics simulation, and enzyme kinetics identified ZINC84525623 as a potential inhibitor of NDM-1. *Int. J. Mol. Sci.* 20 (4). <https://doi.org/10.3390/ijms20040819>.

Roos, K., Wu, C., Damm, W., Reboul, M., Stevenson, J.M., Lu, C., Harder, E.D., 2019. OPLS3e: Extending Force Field Coverage for Drug-Like Small Molecules. *J. Chem. Theory Comput.* 15 (3), 1863–1874. <https://doi.org/10.1021/acs.jctc.8b01026>.

Sagredo, E.A., Blanco, A., Sagredo, A.I., Pérez, P., Sepúlveda-Hermosilla, G., Morales, F., Armisen, R., 2018. ADAR1-mediated RNA-editing of 3'UTRs in breast cancer. *Biol. Res.* 51 (1), 36. <https://doi.org/10.1186/s40659-018-0185-4>.

Suzuki, T., Ueda, H., Okada, S., Sakurai, M., 2015. Transcriptome-wide identification of adenosine-to-inosine editing using the ICE-seq method. *Nat. Protoc.* 10 (5), 715–732. <https://doi.org/10.1038/nprot.2015.037>.

Wulff, B. E., and Nishikura, K., 2010. Substitutional A-to-I RNA editing. *Wiley Interdisciplinary Reviews: RNA*. NIH Public Access. <https://doi.org/10.1002/wrna.10>.

Yang, C.C., Chen, Y.T., Chang, Y.F., Liu, H., Kuo, Y.P., Shih, C.T., Tan, B.C.M., 2017. ADAR1-mediated 3' UTR editing and expression control of antiapoptosis genes fine-tunes cellular apoptosis response. *Cell Death Dis.* 8, (5). <https://doi.org/10.1038/cddis.2017.12> e2833.

Zipeto, M.A., Court, A.C., Sadarangani, A., Delos Santos, N.P., Balaian, L., Chun, H.J., Jamieson, C.H.M., 2016. ADAR1 Activation Drives Leukemia Stem Cell Self-Renewal by Impairing Let-7 Biogenesis. *Cell Stem Cell* 19 (2), 177–191. <https://doi.org/10.1016/j.stem.2016.05.004>.